Electronic Supplementary Material (ESI) for Physical Chemistry Chemical Physics.

Supplementary Information for:

Multiphoton characterization and live cell imaging using fluorescent adenine analogue 2CNqA

J. R. Nilsson[1], C. Benitez-Martin[1], H. G. Sansom[2], P. Pfeiffer[1], T. Baladi[3], Hoang-Ngoan Le[3], A. Dahlén[3], S. W. Magennis[2], and L. M. Wilhelmsson[1,*]

[1] Department of Chemistry and Chemical Engineering, Chalmers University of Technology, Gothenburg SE-412 96, Sweden.
[2] School of Chemistry, University of Glasgow, University Avenue, Glasgow, G12 8QQ, UK.
[3] Oligonucleotide Discovery, Discovery Sciences, R&D, AstraZeneca, Gothenburg, Sweden.
* To whom correspondence should be addressed. Tel: +46-31-772 3051,
Email: marcus.wilhelmsson@chalmers.se.

Content

ENTRY **PAGE**

1. Synthesis of 2CNqATP 2
2. Details on sample preparation and ASO-RNA hybridization for spectroscopy 6
3. Fluorescence quantum yield and lifetime of 2CNqATP 7
4. Determination of multiphoton absorption cross section, multiplicity, and emission spectra 9
5. Photophysical properties of 2CNqA-1 and 2CNqA-2 bound to RNA 10
6. Fluorescence correlation spectroscopy 11
7. In-cell 1P *vs.* 2P intensity comparison using optical sectioning 12
8. 1P *vs.* 2P photobleaching kinetics of 2CNqA 13
9. References 13

1. Synthesis of 2CNqATP

The synthetic route towards 2CNqATP is outlined in Fig. S1. Starting material (**1**) was synthesized as detailed by Wypijewska *et al*.[1], and the succinylated support (**2**) was prepared according to Baladi *et al*.[2].

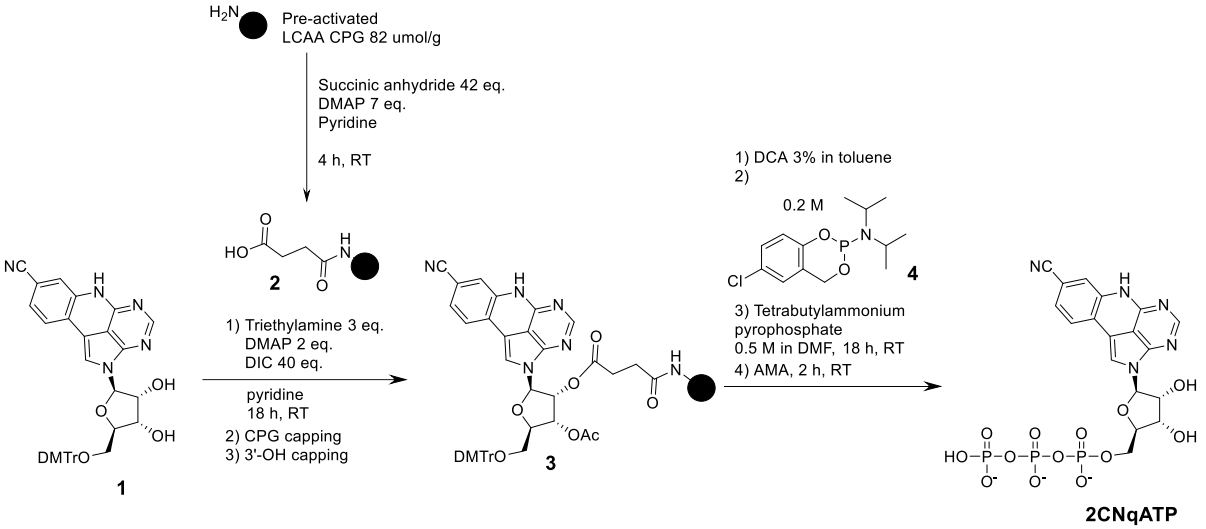

Figure S1. Synthesis scheme for 2CNqATP.

CPG-supported 2-(5-O-(4,4'-Dimethoxytrityl)-β-D-ribofuranosyl)-2,6-dihydro-2,3,5,6-tetraazaaceanthrylene-8-carbonitrile (3). In a 10 mL syringe with PTFE filter, succinylated support (**2**, 0.400 g, 82 µmol/g, 0.033 mmol), DMAP (8 mg, 0.07 mmol), DIC (203 µl, 1.31 mmol), 2CNqA nucleoside (**1**, 0.022 g, 0.033 mmol) and triethylamine (14 µl, 0.10 mmol) were suspended in pyridine (3 mL). The mixture was gently shaken for 18 h at RT. After 18 h, the syringe was purged and the support was washed with pyridine (5 mL), dichloromethane (5 mL) and diethyl ether (10 mL). Subsequently, in the same syringe, DMAP (8 mg, 0.07 mmol), DIC (203 µl, 1.31 mmol), triethylamine (14 µl, 0.10 mmol) and 2,3,4,5,6-pentachlorophenol (0.87 g, 0.33 mmol) were added to the support and the mixture was again suspended in pyridine (3 mL). This was gently shaken for an additional 4 h at RT before a solution of piperidine (2 mL, 20% in DMF, for capping of the unreacted carboxylic acids on the support) was added for 1 min (note that longer exposure time will reduce loading as piperidine cleaves the ester bonds with the nucleoside), and then quickly washed away with DMF (3 x 5 mL), dichloromethane (5 mL) and diethyl ether (5 mL). Finally, the resin was shaken in a CAP A + CAP B mix (50/50 v/v) for 2 h under argon atmosphere, then washed with DMF (5 mL), dichloromethane (5 mL), diethyl ether (5 mL) and argon-dried (final loading: 16 µmol/g, as determined by measuring absorption of a DMTr solution cleaved from a weighed amount of support; molar absorptivity = 70 000 $M^{-1}cm^{-1}$ at 498 nm). Final loading can be increased by performing a second coupling with **1** in the same conditions before capping (typical loading after second coupling 20–25 µmol/g). Concentrating the reaction mixture and washing the residue multiple times with water and diethyl ether allows recovery of nearly 85% of unreacted nucleoside.

((2R,3S,4R,5R)-5-(8-cyano-2,3,5,6-tetraazaaceanthrylen-2(6H)-yl)-3,4-dihydroxytetrahydrofuran-2-yl)methyl hydrogen triphosphate (2CNqATP). Reaction was performed in a 5 mL syringe with a PTFE filter loaded with the CPG-bound 2CNqA nucleoside (**3**, 400 mg, 0.0064 mmol) under an argon atmosphere and shaking. Steps were performed as follows:

a. *5'-DMT removal:* the support was washed with a flow of DCA deblock until the filtrate was colorless, whereafter it was washed with AcN (5 x 5 mL).
b. *Coupling: N,N*-diisopropyl-4H-benzo[d][1,3,2]dioxaphosphinin-2-amine (**4**, 345 mg, 1.36 mmol) was dissolved in 4.8 mL AcN and reacted portion wise with the support (3 equally charged couplings with reaction times 60 s, 60 s, and 90 s, respectively). To each coupling, BTT activator (2.4 mL) was also added. The support was subsequently washed with AcN (3 x 5 mL).
c. *Oxidation:* Pyridine/Water/Iodine (9/1/12.7 v/v/w, 5 mL) for 45 s, followed by AcN wash (3 x 5 mL) and drying of the support in an argon flow.
d. *Triphosphorylation:* Two injections of bis(tetrabutylammonium) dihydrogen diphosphate (0.5 M, 5 ml) were carried out and allowed to react for 15 min and 18 hours, respectively. The support was subsequently rinsed with DMF (5 mL), water (3 x 5 mL), AcN (5 mL) and then dried in an argon flow.
e. *Cleavage and Purification:* Cleavage of the triphosphate was done with AMA (50/50 v/v mix of 23% aq. NH_4OH and 40% aq. methylamine, 5 mL) for 2 h at RT. After 2 h, the AMA filtrate was purged in a round-bottom flask and the support was rinsed 3 times with 23% aq. NH_4OH solution. After freeze-drying the mixture, purification was performed using HPLC with a Waters Atlantis T3 19 x 150 mm column. Elution was achieved using A: 50 mM NH_4OAc in water, and B: AcN (100% A for 2 min, then linear gradient 0%–15% B in 14 min at 30 mL/min), which furnished 2CNqATP (2.3 mg, 55%, as determined by UV absorption) as a light-yellow solid (ammonium salt). m/z calculated for $C_{18}H_{19}N_5O_{13}P_3$ $[M^+H]^+$: 606.0192, found: 606.0170. ^1H NMR (500 MHz, D_2O) δ 7.88 (s, 1H), 7.47 (s, 1H), 7.34 (d, *J* = 7.9 Hz, 1H), 6.99 (d, *J* = 7.8 Hz, 1H), 6.83 (s, 1H), 6.04 (d, *J* = 5.8 Hz, 1H), 4.76 (s, 1H), 4.61 (s, 1H), 4.39 (s, 1H), 4.31 (s, 2H).^{31}P NMR (202 MHz, D_2O) δ -22.48 (bs, 1P), -11.19 (d, J=19.9 Hz, 1P), -9.25 (bs, 1P).

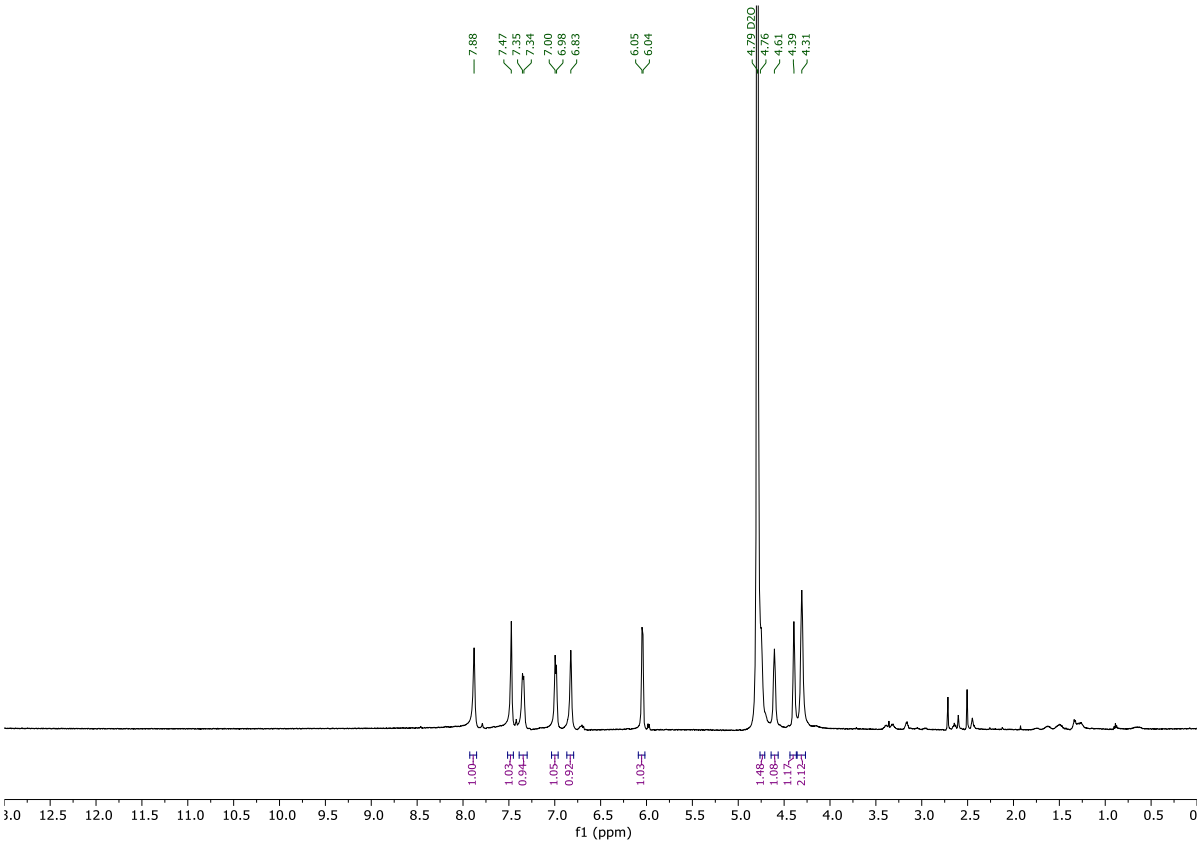

Figure S2. ^{1}H NMR (500 MHz, D_2O) spectrum of 2CNqATP.

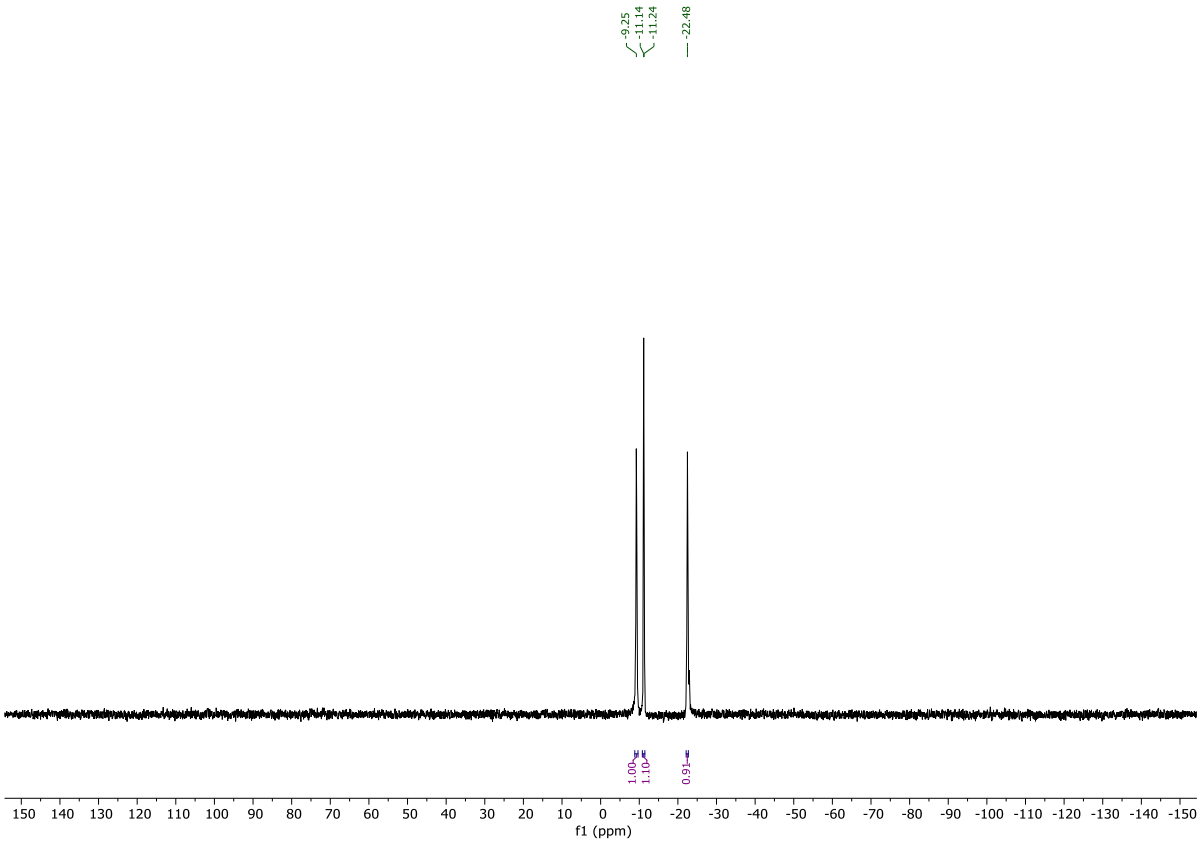

Figure S3. ^{31}P NMR (202 MHz, D_2O) spectrum of 2CNqATP.

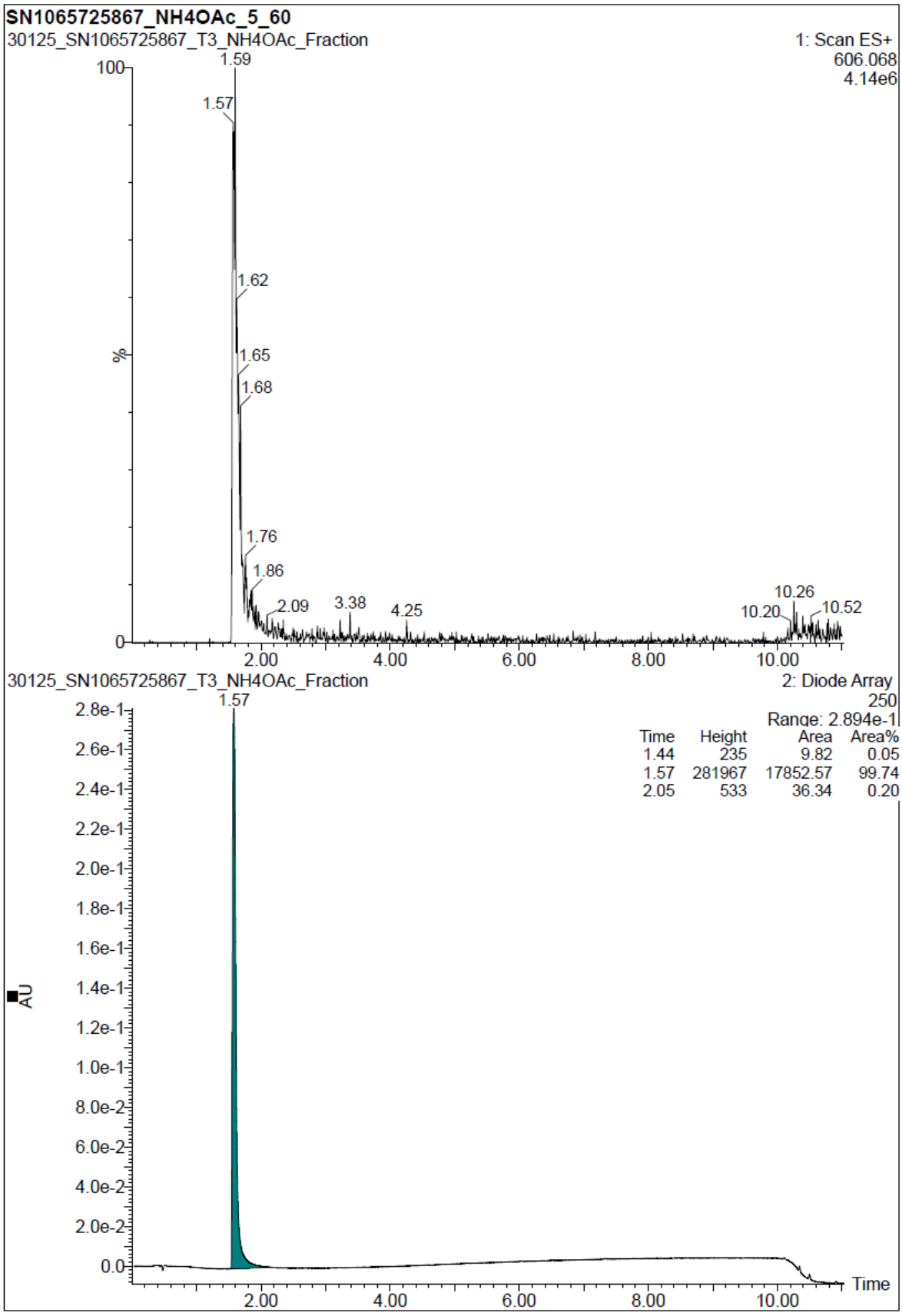

Figure S4. HPLC-MS (ESI-TOF) of 2CNqATP. Analytical HPLC method: Waters Aquity HSS T3 2.1 x 50 mm column; elution was achieved using A: 50 mM NH_4OAc in water, and B: AcN (linear gradient 5%–60% B in 9.3 min at 0.4 mL/min, 45 °C). UV purity 99.7%.

2. Details on sample preparation and ASO-RNA hybridization for spectroscopy.

For all experiments except the fluorescence correlation spectroscopy (detailed in the manuscript experimental section), the 2CNqATP was measured in phosphate buffer (pH 7.2) containing additional NaCl and KCl (1XDPBS (no magnesium, no calcium) buffer purchased from Gibco), and the ASOs were measured in a 10 mM phosphate buffer (pH 7.4) containing 1.0 mM EDTA and 100 mM NaCl. The EDTA was included in the ASO buffer to suppress the activities of metal cation-dependent degradative enzymes. The 1P absorption, relative emission (the area of which represents the relative fluorescence quantum yields), and fluorescence lifetimes of the 2CNqA fluorophore were found to be very similar in all three buffer systems (Fig. S5).

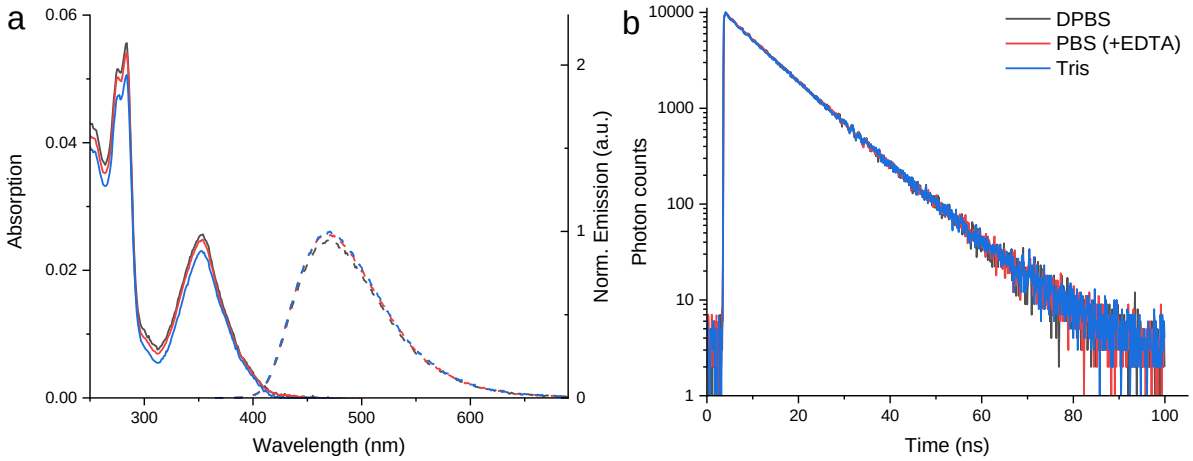

Figure S5. Comparison of 1P absorption, relative emission, and fluorescence lifetime of 2CNqATP in the three buffer systems detailed in the text above, *i.e.*, commercial 1XDPBS (black), PBS + EDTA (red), and Tris buffer (blue). **a)** Solid lines: UV-vis absorption spectra of a 0.5 mM mQ water stock solution diluted to a final concentration 10 µM in the specified buffer. Dashed lines: Emission spectra of the same solutions, divided by the absorption at the excitation wavelength (350 nm). All emission spectra were subsequently scaled by the same factor to match the intensity of the absorption band. **b)** Fluorescence decays measured using time-correlated single photon counting.

The oligonucleotide molar absorptivities at 260 nm (L[mol oligonucleotide]$^{-1}$cm^{-1}) were calculated using a base composition method in which the following single nucleobase absorptivities were adopted: adenine: 15 300 M^{-1}cm^{-1}, thymine or uracil: 9 300 M^{-1}cm^{-1}, guanine: 11 800 M^{-1}cm^{-1}, cytosine 7 400 M^{-1}cm^{-1}, and 2CNqA: 14 600 M^{-1}cm^{-1}. The final oligonucleotides absorptivities were arrived at by multiplying the sum of the nucleobase absorptivities by a factor of 0.9, to account for the hypochromic base stacking effect. The RNA that is complementary to the ASO sequences, *i.e.* having nucleobase sequence: 5'-GCUGCUAUUAGAAUGC-3', was purchased from Sigma. The ASO:RNA duplexes were afforded by first mixing the single-strands at a 1:1.3 ASO:RNA ratio at RT (*ca.* 22 °C), then annealing them using the following temperature program: RT to 85 °C at 4 °C/min, remain at 85 °C for 15 min, 85°C to RT at 1.5 °C/min. The 30% excess of RNA in the preparation was used to promote full hybridization of the ASOs. The final single-strand or duplex concentrations were in the range 7–10 µM, and accurately determined using UV-vis spectroscopy.

3. Fluorescence quantum yield and lifetime determination of 2CNqATP

Fluorescence quantum yield (Φ_F) determination of 2CNqATP was performed in a 3.0 mm × 3.0 mm path length quartz cuvette and a sample volume of *ca.* 70 µL, using the absorption and emission spectrophotometer setup described in the manuscript. The Φ_F was determined relative to a solution of quinine sulphate in 0.5 M H_2SO_4 ($\Phi_{F,REF}$ = 55%) and calculated according to Eq. S1.

$$\Phi_F = \Phi_{F,REF} \times \frac{\int I_S(\lambda)d\lambda}{\int I_{REF}(\lambda)d\lambda} \times \frac{A_{REF}}{A_S} \times \frac{\eta_S^2}{\eta_{REF}^2} \quad \text{(Eq. S1)}$$

where $I_S(\lambda)$ and $I_{REF}(\lambda)$ denote the emission intensity of the sample and reference, respectively. The absorption at the excitation wavelength (350 nm) for the sample (A_S) and reference (A_{REF}) were below 0.02 to avoid inner filter effects. The adopted solvent refractive index for the sample and reference were η_S = 1.333 (phosphate buffer) and η_{REF} = 1.339 (for 0.5 M H_2SO_4), respectively. The presented quantum yield is given as the mean of two independent replicates with Φ_F = 0.465 and 0.472 (S.D. = 0.004). The absorption and emission spectra of 2CNqATP are shown in Fig. S5.

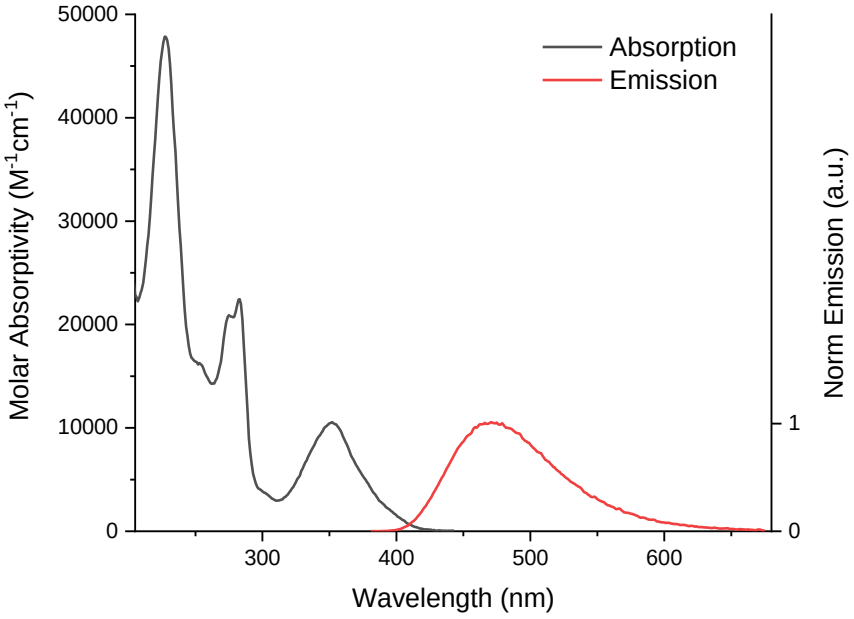

Figure S6. Absorption and normalized emission spectra of 2CNqATP in 1X Dulbecco's phosphate-buffered saline, pH 7.2.

The fluorescence lifetime of 2CNqATP was determined using a time-correlated single photon counting setup. The sample, contained in a 3.0 mm × 3.0 mm path length quartz cuvette at a sample volume of *ca.* 70 µL, was excited using an LDH-P-C-375 (PicoQuant) pulsed laser diode with emission centered at 377 nm. Full width at half maxima of the pulse were *ca.* 1 nm and 70 ps for wavelength and time, respectively. The laser diodes were powered by a PDL 800-B (PicoQuant) laser driver delivering light pulses at a frequency of 10 MHz. Sample emission was collected at a right angle, through a polarizer set at 54.7° (magic angle detection) and observed at 460 nm with a 10 nm bandpass. Photon counts were recorded on a R3809U-50 microchannel plate PMT (Hamamatsu) and fed into a LifeSpec

multichannel analyzer (Edinburgh Instruments) with 1024 channels (at 98 ps/channel resolution) until the stop condition of 10^4 counts in the top channel was met. The instrument response function (IRF) was determined using a frosted glass (scattering) insert. A least-square fitting procedure with IRF re-convolution was carried out by the DecayFit software (DecayFit - Fluorescence Decay Analysis Software 1.3, FluorTools, www.fluortools.com), using equation S2:

$$I(t) = \int_0^t IRF(t') \sum_{i=1}^{n} \alpha_i e^{-\frac{t-t'}{\tau_i}} dt' \qquad \text{(Eq. S2)}$$

The decays were satisfactorily fit to a monoexponential expression (n = 1). The lifetime reported herein is given as the mean of two independent replicates with τ_f = 9.85 ns and 9.86 ns (S.D. = 0.005); the sample decay, IRF, and fitted data of one replicate is shown in Fig. S6.

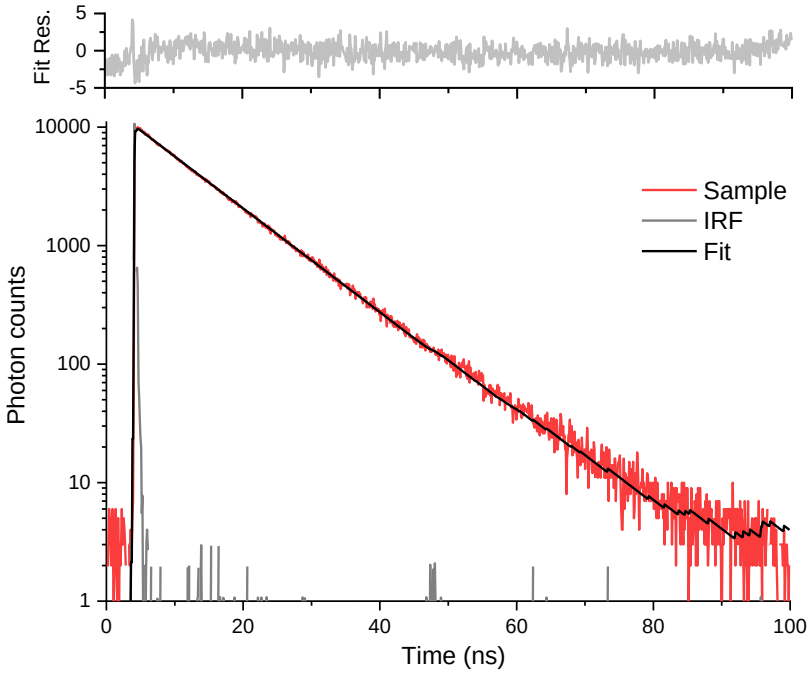

Figure S7. Fluorescence lifetime determination of 2CNqATP in 1X Dulbecco's phosphate-buffered saline, pH 7.2 using time-correlated single photon counting. Bottom panel: Sample decay, IRF and monoexponential fit. Top panel: Fitting residual.

4. Determination of multiphoton absorption cross section, multiplicity, and emission spectra

The multiphoton absorption properties were determined using the microscopy instrumentation described in the Methods and Materials section in the manuscript. The samples were enclosed in a cover slip sandwich using a custom-made cover slip holder, also capturing an air bubble adjacent to the sample solution for assessing the background signal (*vide infra*).

The $\sigma_{2PA}(\lambda)$ were determined relative to a solution of rhodamine 6G in methanol ($\Phi_{F,REF}$ = 94%; $\sigma_{2PA,REF}(\lambda)$ adopted from de Reguardati *et al.*[3]), using the two-photon-induced-fluorescence method, and calculated according to equation S3.[4, 5]

$$\sigma_{2\mathrm{PA}}(\lambda) = \sigma_{2\mathrm{PA,REF}}(\lambda) \times \frac{\mathrm{I_S} - \mathrm{I_B}}{\mathrm{I}_{REF} - \mathrm{I_B}} \times \frac{\mathrm{C_{REF}}}{\mathrm{C_S}} \times \frac{\eta_{\mathrm{REF}}}{\eta_{\mathrm{S}}} \times \frac{\Phi_{\mathrm{F,REF}}}{\Phi_{\mathrm{F,S}}} \qquad \text{(Eq. S3)}$$

Here, I_S, I_B, and I_{REF} denote the mean intensity per area of the sample, background (air), and reference, respectively, which were determined by acquiring microscopy images of both sides of the air/liquid sample boundary in the same field of view. The concentrations of the samples (C_s, in the range 7–10 µM) and reference (C_{REF} = 0.290 µM) were accurately determined using UV-vis spectroscopy prior to the experiment. The adopted solvent refractive indices for the sample and reference were η_S = 1.333 (water) and η_{REF} = 1.328 (methanol), respectively. The fluorescence quantum yields of the samples, $\Phi_{F,S}$, were adopted from Nilsson *et al.*[6] for all compounds except 2CNqATP, for which it was determined in this study (see supplementary information section 3). All σ_{2PA} were determined on two separate independent occasions and are presented as the mean value, with each pair of replicates differing by no more than 10%.

2P-induced emission spectra were determined by exciting at 700 nm while scanning the acousto-optical tunable emission filters in the microscope between 420–690 nm in intervals of 10 nm. All emission data in the σ_{2PA} determination and 2P emission spectra were corrected for the detector spectral response (quantum efficiency *vs.* wavelength data provided by the instrument manufacturer) in the applied emission range.

To determine the multiplicity of the absorption process, emission was recorded as detailed above at different excitation intensities, and the integrated emission in the emission wavelength range were plotted as a function of relative excitation power for each of the samples.

5. Photophysical properties of 2CNqA-1 and 2CNqA-2 bound to RNA.

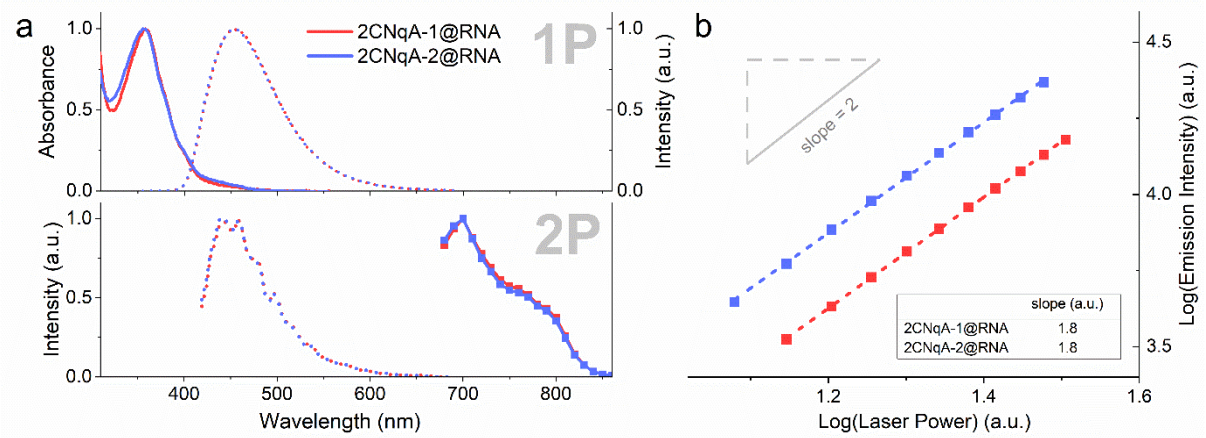

Figure S8. Photophysical properties of 2CNqA-1 (red) and 2CNqA-2 (blue), when bound to RNA. **a)** Top panel: Normalized 1P absorption spectra (solid lines) and emission spectra (dotted lines, λ_{exc} = 350 nm). Bottom panel: Normalized emission spectra (dotted lines, λ_{exc} = 700 nm) and 2P cross section absorption spectra (boxed solid lines, λ_{em} = 460 nm). **b)** Absorption multiplicity plot, where integrated emissions were determined at various excitation intensities (λ_{exc} = 700 nm). Linear regressions (dashed lines, see supplementary information Table S1 for details on fitting) resulted in the slopes depicted in the table inset.

The cross sections for the RNA-bound 2CNqA-1 and 2CNqA-2 at their maxima (700 nm) are 7.0 GM and 13 GM, respectively, while the absorption multiplicities are 1.8 for both ASO duplexes. The fitting parameters resulting from the linear regressions used to analyze the intensity log–log plots (Fig 2b and Fig S6b) are summarized in Table S1.

Table S1. Fitting parameters for the intensity log–log plots shown in Fig. 2b and Fig. S7b. Slope and intercept are shown as fitted value ± standard error. COD = coefficient of determination.

Compound	slope	intercept	R^2 (COD)
2CNqA-1	1.86 ± 0.01	1.63 ± 0.01	0.9998
2CNqA-1@RNA	1.83 ± 0.02	1.43 ± 0.02	0.9999
2CNqA-2	1.84 ± 0.02	1.64 ± 0.02	0.9993
2CNqA-2@RNA	1.82 ± 0.02	1.70 ± 0.02	0.9995
2CNqATP	1.87 ± 0.01	1.89 ± 0.01	0.9998

6. Fluorescence correlation spectroscopy

The fluorescence correlation data (Fig. 3) were fitted to a single-component diffusion model (Eq. S4):

$$G(t) = \frac{\left(1-\frac{I_B}{S}\right)^2}{\sqrt{8N}}\left(1+\frac{t}{\tau_D}\right)^{-1}\left(1+k^2\frac{t}{\tau_D}\right)^{-\frac{1}{2}} \qquad \text{(Eq. S4)}$$

where I_B is the background intensity, S is the total signal intensity, τ_D is the diffusion time and $k = \omega_0/z_0$ (ω_0 is the 1/e radius of the point spread function perpendicular to the beam and z_0 is the 1/e radius parallel to the beam).

Table S2. Fitting parameters for all replicates in the FCS.

Compound	I_B (kHz)	S (kHz)	N	τ_D (µs)	k
2CNqA-1	0.36	7.69	8.32	53	4.40
	0.36	7.72	8.28	53	4.40
	0.36	8.27	6.91	44	4.40
2CNqATP	0.35	16.59	5.75	34	4.40
	0.35	21.68	7.51	34	4.40
	0.35	21.57	8.61	39	4.40
	0.35	21.51	8.41	36	4.40

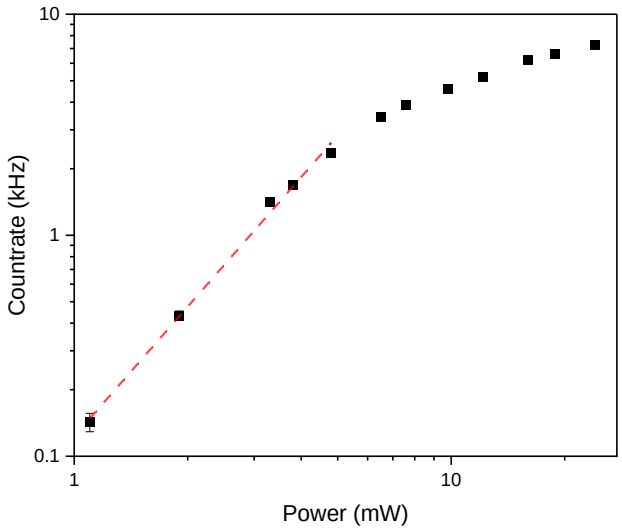

Figure S9. Power series of a 100 nM sample of 2CNqA-1 using the broadband multiphoton setup. The gradient of the linear region is 1.95 ± 0.08 confirming a 2P process. Onset of saturation is around 6 mW. No higher-order processes were observed. Note that the full laser spectrum was used for this measurement (220 nm FWHM centered on 800 nm).

7. In-cell 1P *vs.* 2P intensity comparison using optical sectioning

For the 1P *vs.* 2P intracellular intensity comparison, a set of images of cells exposed to 2CNqA-1, 2CNqA-2, or buffer (control) were acquired using optical sectioning (z-stacks). Each image stack was initiated in an x-y focal plane immediately above the cells and parallel to the cover glass surface on which the cells were adhered. Scanning then proceeded successively through the cell layer with a change in z-distance of 2 µm per image (*i.e.,* $\Delta x = \Delta y = 0$, $\Delta z = -2$ µm), and a total of seven images per imaging mode (*i.e.* brightfield, 1P, and 2P) and stack were acquired. The total z-range of the stack is (7-1) × 2 µm = 12 µm, which was sufficient to scan through the full thickness of the cell layer. The ensuing image analysis procedure is described in Fig S10. The result of the intracellular intensity quantification is shown in Fig. S11.

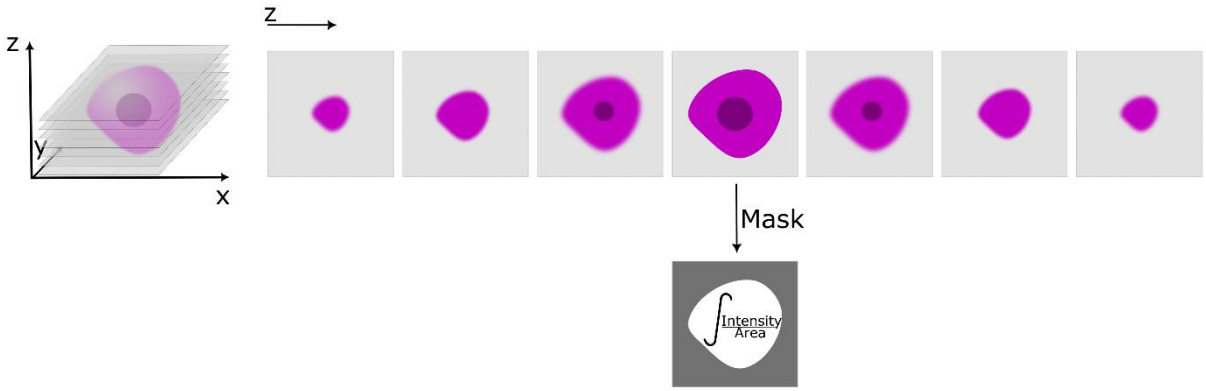

Figure S10. Z-stack image processing and analysis. After acquiring the image stacks, each containing seven images per imaging mode (*i.e.,* brightfield, 1P, and 2P) at different z-positions in the cell, a binary mask (extracellular = 0, intracellular =1) was created by manually tracing the cell membrane/medium boundary in the brightfield image. The mask was then applied to (multiplied by) the 1P and 2P images, whereafter the total intensity per intracellular area unit was evaluated and summed up for all seven images in the stack.

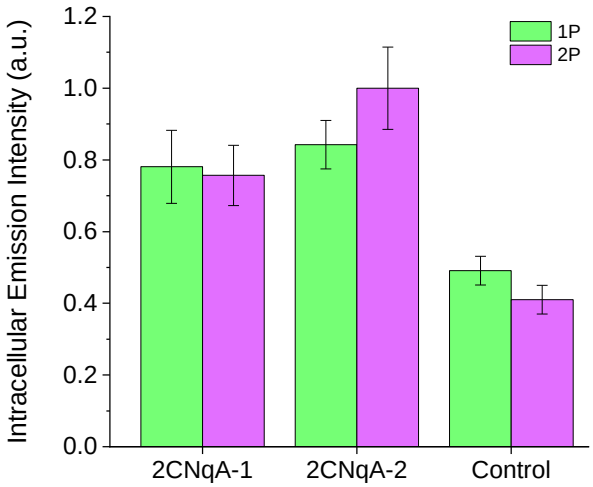

Figure S11. Normalized total intracellular intensity per area unit evaluated using fluorescence microscopy optical sectioning of live Huh7 cells exposed to 3.0 µM 2CNqA-1 or 2CNqA-2 at 37 °C for 24 h; Control cells were exposed to buffer only. Samples were excited with a continuous 405 nm diode laser for 1P and a pulsed laser at 750 nm for 2P. Identical emission filters (λ_{em} = 410–680 nm) and detector settings were used for the 1P and 2P images. The image acquisition and analysis are described in the section 7 text and Fig S10, respectively. Data are presented as the mean (± S.D.) of five stacks (for 2CNqA-1 and 2CNqA-2) or three stacks (for control).

8. 1P *vs.* 2P photobleaching kinetics of 2CNqA

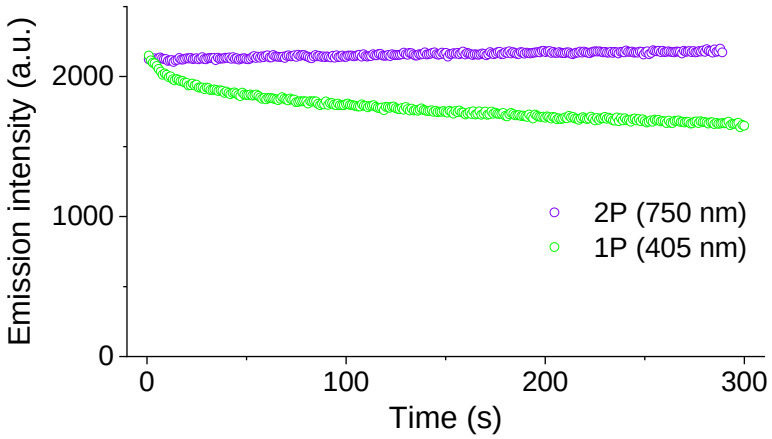

Figure S12. Photobleaching kinetics of 2CNqATP (10 µM) in DPBS buffer during continuous microscopy image acquisition using first 2P, then 1P excitation. Excitation settings were comparable to those used in the cell imaging in this work, albeit with laser powers slightly adjusted to render the same emission intensity at t = 0; all other acquisition parameters were identical for the two imaging modes. The presented data is the integrated emission intensity from an identical region of interest in the time-lapses.

9. References

1. A. Wypijewska del Nogal, A. F. Füchtbauer, M. Bood, J. R. Nilsson, M. S. Wranne, S. Sarangamath, P. Pfeiffer, V. S. Rajan, A. H. El-Sagheer, A. Dahlén, T. Brown, M. Grøtli and L. M. Wilhelmsson, *Nucleic Acids Res.*, 2020, **48**, 7640-7652.
2. T. Baladi, J. R. Nilsson, A. Gallud, E. Celauro, C. Gasse, F. Levi-Acobas, I. Sarac, M. R. Hollenstein, A. Dahlén, E. K. Esbjörner and L. M. Wilhelmsson, *J. Am. Chem. Soc.*, 2021, **143**, 5413-5424.
3. S. de Reguardati, J. Pahapill, A. Mikhailov, Y. Stepanenko and A. Rebane, *Opt. Express*, 2016, **24**, 9053-9066.
4. M. Rumi and J. W. Perry, *Adv. Opt. Photon.*, 2010, **2**, 451-518.
5. F. Terenziani, C. Katan, E. Badaeva, S. Tretiak and M. Blanchard-Desce, *Adv. Mater.*, 2008, **20**, 4641-4678.
6. J. R. Nilsson, T. Baladi, A. Gallud, D. Baždarević, M. Lemurell, E. K. Esbjörner, L. M. Wilhelmsson and A. Dahlén, *Sci. Rep.*, 2021, **11**, 11365.